Polymer Journal (2012) 44, 1071–1076

www.nature.com/pj

ORIGINAL ARTICLE

Chiral amplification in double-stranded helical polymers through chiral and achiral amidinium–carboxylate salt bridges

Wataru Makiguchi, Shinzo Kobayashi, Yoshio Furusho[1] and Eiji Yashima

A series of *m*-terphenyl-based random copolymers of chiral and achiral amidines, and their complementary homopolymers of achiral carboxylic acids were prepared by the copolymerization of a *p*-diiodobenzene derivative, with the diethynyl monomers containing a chiral or achiral amidine group and a carboxyl group using the Sonogashira coupling reaction. The obtained chiral/achiral amidine copolymers assembled into a double-stranded helical structure upon complexation with the complementary achiral homopolymer of carboxylic acids through interstrand amidinium–carboxylate salt bridges. The complexes exhibited characteristic induced cotton effects in the π-conjugated main-chain chromophore regions, indicating that the interstrand duplexes possess a preferred-handed double-helical structure. The effect of the chiral and achiral amidine contents on the amplification of the helical chirality ('the sergeants and soldiers effect') during the interstrand double-helix formation was investigated by comparing the cotton effect patterns and intensities of the duplexes with those of the corresponding all-chiral amidine-based double-helical polymer.
Polymer Journal (2012) **44,** 1071–1076; doi:10.1038/pj.2012.70; published online 16 May 2012

Keywords: amidine; carboxylic acid; chirality; chiral amplification; circular dichroism; double helix

INTRODUCTION

The complementary double-helical structure of DNA is a key structural motif for its vital functions in biological systems, such as replication and the storage of genetic information, which has prompted chemists to develop synthetic double-helical polymers and oligomers (foldamers).[1–3] Although a large number of single-stranded helical polymers and oligomers have been reported,[2–12] examples of double-stranded helical polymers and oligomers remain relatively scarce.[2,3,8,9,13–22] We have recently reported on the rational design and synthesis of a series of complementary double-stranded helical oligomers[23–28] with an optical activity that consists of a crescent-shaped *m*-terphenyl-based backbone containing amidine and carboxylic acid groups. In our design, the formation of the intertwined duplex is driven by the formation of an amidinium–carboxylate salt bridge, and the helicity of the duplexes can be readily controlled by the introduction of chiral substituents on the nitrogen atoms of the amidine residues.[9,15,18,19] We also reported on *m*-terphenyl-based conjugated polymers, which contain optically active amidine groups (poly-A_1) and achiral carboxylic groups (poly-C), that folded into an intertwined double-stranded helical structure through the chiral amidinium–carboxylate salt bridges.[29]

In this study, we synthesized a series of *m*-terphenyl-based random copolymers containing chiral and achiral amidines (poly-A_x) and their complementary homopolymers containing achiral carboxylic acids (poly-C), and investigated the effect of the chiral/achiral amidine contents on the amplification of the helical chirality[30,31] during the complementary double-helix formation ('the sergeants and soldiers effect')[3,4,32,33] (Figure 1) using absorption and circular dichroism (CD) spectroscopies. Such a unique amplification of the helical chirality along the polymer backbones assisted by a small chiral unit has been proven to be applicable to some stiff single-stranded helical polymers[3,7,9,31–39] and supramolecular helical systems.[30,40–44] In some artificial double-stranded helical oligomers, an excess of the one-handed helical structure was produced by a small number of chiral units that were introduced into an achiral strand.[22,45–47] However, the amplification of the helical chirality in the double-stranded helical polymers based on 'the sergeants and soldiers effect' has not been reported, except for oligomers.[28]

EXPERIMENTAL PROCEDURE

Instruments

^{1}H nuclear magnetic resonance (NMR) spectra were obtained using a Varian UNITY INOVA 500AS spectrometer (Varian, Palo Alto, CA, USA) operating at 500 MHz. Chemical shifts are reported in parts per million (δ) downfield from tetramethylsilane, which was used as the internal standard, in $CDCl_3$. The elemental analyses were performed by the Laboratory of Elemental Analyses in

Department of Molecular Design and Engineering, Graduate School of Engineering, Nagoya University, Nagoya, Japan
[1]Current address: Molecular Engineering Institute, Kinki University, 11–6, Kayanomori, Iizuka, Fukuoka 820–8555, Japan.
Correspondence: Professor E Yashima, Department of Molecular Design and Engineering, Graduate School of Engineering, Nagoya University, Chikusa-ku, Nagoya 464–8603, Japan.
E-mail: yashima@apchem.nagoya-u.ac.jp
Received 3 March 2012; revised 8 March 2012; accepted 10 March 2012; published online 16 May 2012

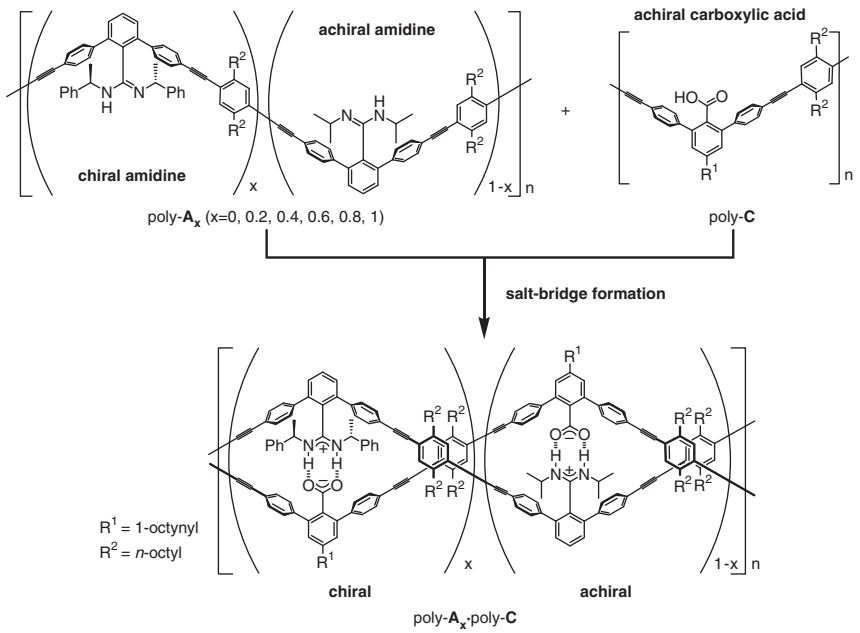

Figure 1 Formation of the complementary double-stranded helical polymers composed of chiral/achiral amidine strands and an achiral carboxylic acid strand through interstrand amidinium–carboxylate salt bridges.

the Department of Agriculture, Nagoya University. The infrared (IR) spectra were recorded using a JASCO Fourier Transform IR-680 spectrophotometer (Jasco, Hachioji, Japan). The absorption and CD spectra were measured in a 1.0-mm quartz cell on a JASCO V-570 spectrophotometer (Jasco) and a JASCO J-820 spectropolarimeter, (Jasco) respectively. The temperature was controlled with a JASCO PTC-423L apparatus (Jasco). The size-exclusion chromatography measurements were performed with a JASCO PU-2080 liquid chromatograph equipped with an ultraviolet–visible (254 nm; JASCO ultraviolet-2070) detector. Two Tosoh (Tokyo, Japan) TSKgel Multipore H_{XL}-M size-exclusion chromatography columns (30 cm) were connected in series using tetrahydrofuran (THF)-containing tetrabutylammonium bromide (0.1 wt%) and THF-containing triethylamine (50 mM) as the eluents for poly-C and poly-A_x, respectively, at a flow rate of 1.0 ml min^{-1}. The molecular weight calibration curves were obtained from polystyrene standards (Tosoh).

Materials

All reagents and dehydrated solvents were purchased from Aldrich (Milwaukee, WI, USA), Wako Pure Chemical Industries (Osaka, Japan) or Tokyo Chemical Industry (TCI, Tokyo, Japan) unless otherwise noted. Chiral and achiral amidines and carboxylic acid monomers ((*R*)-A, A, and C, respectively) were prepared according to previously reported methods.[29]

Polymerization

Using previously reported methods, poly-A_x and poly-C were synthesized from (*R*)-A and A and C by copolymerizing with 1,4-diiodo-2,5-dioctylbenzene using the Sonogashira coupling reaction (Scheme 1).[29] The polymerization results are summarized in Table 1.

The spectroscopic data of poly-A_0 are as follows: IR (neat, cm^{-1}): 3433 (ν_{N-H}), 2206 ($\nu_{C\equiv C}$), 1635 ($\nu_{C=N}$). ^{1}H NMR ($CDCl_3$, 50 °C, poly-A_0 (5.7 mM), CH_3CO_2H (23 mM), 500 MHz): δ 0.68–0.98 (m, CH_3, 18H), 1.22–1.48 (m, CH_2, 20H), 1.70–1.80 (m, $ArCH_2CH_2$, 4H), 2.07 (s, CH_3CO_2, 12.1H), 2.65–2.95 (m, $ArCH_2$, 4H), 3.08–3.22 (m, CHN, 2H), 7.41 (s, ArH, 2H), 7.52–7.76 (m, ArH, 11H). Anal. calcd. (%) for $(C_{51}H_{62}N_2 \cdot H_2O)_n$: C, 84.95; H, 8.95; N, 3.88. Found: C, 84.77; H, 8.70; N, 3.72.

The spectroscopic data of poly-$A_{0.2}$ are as follows: IR (neat, cm^{-1}): 3433 (ν_{N-H}), 2206 ($\nu_{C\equiv C}$), 1633 ($\nu_{C=N}$). ^{1}H NMR ($CDCl_3$, 50 °C, poly-$A_{0.2}$ (10 mM), CH_3CO_2H (100 mM), 500 MHz): δ 0.70–0.92 (m, CH_3, 16.76H), 1.18–1.48 (m, CH_2, 20H), 1.67–1.80 (m, $ArCH_2CH_2$, 4H), 2.08 (s, CH_3CO_2, 30H), 2.74–2.94 (m, $ArCH_2$, 4H), 3.11–3.21 (m, CHN, 1.59H), 3.95–4.03 (m, CHN, 0.41H), 6.71–6.78 (m, ArH, 0.83H), 7.04–7.10 (m, ArH, 0.83H), 7.21–7.33 (m, ArH, 2.07H), 7.37–7.44 (m, ArH, 2H), 7.49–7.81 (m, ArH, 9.34H). Anal. calcd. (%) for $(C_{52.85}H_{62.74}N_2)_n$: C, 87.47; H, 8.69; N, 3.84. Found: C, 87.23; H, 8.65; N, 3.84.

The spectroscopic data of poly-$A_{0.4}$ are as follows: IR (neat, cm^{-1}): 3431 (ν_{N-H}), 2204 ($\nu_{C\equiv C}$), 1637 ($\nu_{C=N}$). ^{1}H NMR ($CDCl_3$, 50 °C, poly-$A_{0.4}$ (10 mM), CH_3CO_2H (100 mM), 500 MHz): δ 0.70–0.95 (m, CH_3, 15.44H), 1.20–1.48 (m, CH_2, 20H), 1.66–1.81 (m, $ArCH_2CH_2$, 4H), 2.08 (s, CH_3CO_2, 30H), 2.75–2.91 (m, $ArCH_2$, 4H), 3.12–3.22 (m, CHN, 1.15H), 3.92–4.04 (m, CHN, 0.85H), 6.69–6.80 (m, ArH, 1.7H), 7.02–7.10 (m, ArH, 1.7H), 7.21–7.32 (m, ArH, 4.26H), 7.37–7.43 (m, ArH, 2H), 7.51–7.81 (m, ArH, 7.59H). Anal. calcd. (%) for $(C_{54.67}H_{63.47}N_2)_n$: C, 87.80; H, 8.49; N, 3.71. Found: C, 87.71; H, 8.54; N, 3.51.

The spectroscopic data of poly-$A_{0.6}$ are as follows: IR (neat, cm^{-1}): 3429 (ν_{N-H}), 2204 ($\nu_{C\equiv C}$), 1637 ($\nu_{C=N}$). ^{1}H NMR ($CDCl_3$, 50 °C, poly-$A_{0.6}$ (10 mM), CH_3CO_2H (100 mM), 500 MHz): δ 0.69–0.94 (m, CH_3, 14.20H), 1.16–1.49 (m, CH_2, 20H), 1.66–1.80 (m, $ArCH_2CH_2$, 4H), 2.08 (s, CH_3CO_2, 30H), 2.72–2.95 (m, $ArCH_2$, 4H), 3.11–3.22 (m, CHN, 0.73H), 3.92–4.03 (m, CHN, 1.27H), 6.70–6.80 (m, ArH, 2.53H), 7.04–7.10 (m, ArH, 2.53H), 7.21–7.32 (m, ArH, 6.33H), 7.37–7.43 (m, ArH, 2H), 7.51–7.81 (m, ArH, 5.94H). Anal. calcd. (%) for $(C_{56.74}H_{64.30}N_2)_n$: C, 88.09; H, 8.32; N, 3.58. Found: C, 87.85; H, 8.59; N, 3.63.

The spectroscopic data of poly-$A_{0.8}$ are as follows: IR (neat, cm^{-1}): 3429 (ν_{N-H}), 2204 ($\nu_{C\equiv C}$), 1637 ($\nu_{C=N}$). ^{1}H NMR ($CDCl_3$, 50 °C, poly-$A_{0.8}$ (10 mM), CH_3CO_2H (100 mM), 500 MHz): δ 0.70–0.92 (m, CH_3, 13.11H), 1.18–1.50 (m, CH_2, 20H), 1.66–1.79 (m, $ArCH_2CH_2$, 4H), 2.08 (s, CH_3CO_2, 30H), 2.71–2.91 (m, $ArCH_2$, 4H), 3.12–3.21 (m, CHN, 0.37H), 3.93–4.04 (m, CHN, 1.63H), 6.69–6.80 (m, ArH, 3.26H), 7.02–7.10 (m, ArH, 3.26H), 7.19–7.33 (m, ArH, 8.15H), 7.36–7.42 (m, ArH, 2H), 7.49–7.81 (m, ArH, 4.48H). Anal. calcd. (%) for $(C_{58.93}H_{65.17}N_2)_n$: C, 88.34; H, 8.18; N, 3.48. Found: C, 88.10; H, 8.09; N, 3.38.

CD measurements

The typical experimental procedure for CD measurements is described below. Stock solutions of poly-A_1 (1.0 mM per unit) and poly-C (1.0 mM/unit) in THF were prepared in 3-ml flasks equipped with stopcocks. Four hundred

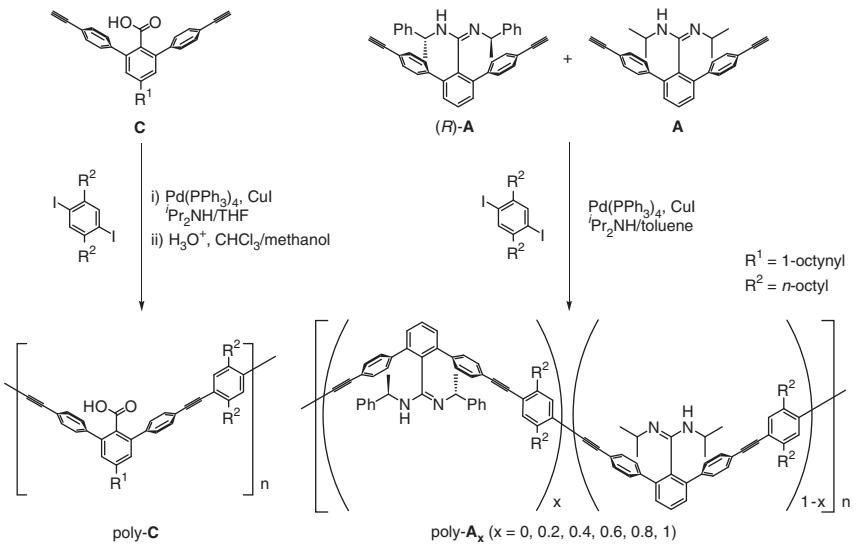

Scheme 1 Synthesis of poly-C and a series of copolymers consisting of chiral/achiral amidine units (poly-A$_x$).

Table 1 Polymerization results[a]

			Polymer			
Run	*Monomer (feed molar ratio)*	*Sample code*	*Yield (%)*[b]	*(R)-A/A (molar ratio)*[c]	$M_n \times 10^{-3}$[d]	M_w/M_n[d]
1	A	poly-A_0	49	—	29	2.1
2	(*R*)-A/A (0.2/0.8)	poly-$A_{0.2}$	57	0.21/0.79	15	2.5
3	(*R*)-A/A (0.4/0.6)	poly-$A_{0.4}$	56	0.43/0.57	9.4	3.4
4	(*R*)-A/A (0.6/0.4)	poly-$A_{0.6}$	65	0.63/0.37	9.6	3.6
5	(*R*)-A/A (0.8/0.2)	poly-$A_{0.8}$	58	0.81/0.19	12	3.7
6	(*R*)-A	poly-A_1	95	—	39	11.6
7	C	poly-C	26	—	22[e]	6.6[e]

[a]Runs 1–6; [Monomer] = [1,4-diiodo-2,5-dioctylbenzene] = 0.05 M, [Pd(PPh$_3$)$_4$] = [CuI] = 0.005 M. Run 7; [C] = [1,4-diiodo-2,5-dioctylbenzene] = 0.025 M, [Pd(PPh$_3$)$_4$] = 6.25×10^{-4} M, [CuI] = 1.25×10^{-3} M.
[b]Runs 1–6, methanol-insoluble part. Run 7, THF-soluble part after acidification.
[c]Estimated by ^{1}H NMR.
[d]Determined by SEC using polystyrene standards.
[e]Determined as its methyl ester.

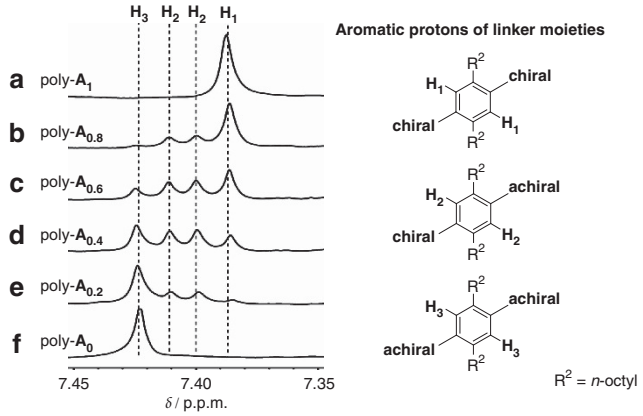

Figure 2 Partial ^{1}H NMR spectra of poly-A$_x$ measured in $CDCl_3$ at 50 °C.

microliter aliquots of the poly-A_1 and poly-C solutions were transferred to 2-ml flasks equipped with stopcocks using a Hamilton microsyringe, and the solutions were then diluted with THF (1.6 ml) to keep the poly-A_1 and poly-C concentrations at 0.2 mM per unit. A 250-µl aliquot of the poly-A_1 solution (0.2 mM per unit) was then transferred to a 1.0-mm quartz cell equipped with a stopcock. A 250-µl aliquot of the poly-**C** solution (0.2 mM per unit) was added to the quartz cell, and the absorption and CD spectra were recorded after mixing. The absorption and CD spectra of mixtures of poly-A$_x$ ($x = 0.2$, 0.4, 0.6 and 0.8) and poly-C were measured in the same way.

RESULTS AND DISCUSSION

m-Terphenyl-based chiral *N,N′*-bis((*R*)-1-phenylethyl)amidine ((*R*)-A) and achiral *N,N′*-diisopropylamidine (A) monomers and an achiral carboxylic acid monomer (C) were synthesized and copolymerized with 1,4-diiodo-2,5-dioctylbenzene using the Sonogashira coupling reaction according to the previously reported methods (Scheme 1).[29] The polymerization results are summarized in Table 1. Except for poly-C, all of the homopolymers and copolymers were obtained in moderate yields (>49%) and had relatively high molecular weights ($M_n > ca.\ 10 \times 10^3$). The rather low yield of poly-C was due to the poor solubility of its high-molecular-weight component that was insoluble in common organic solvents after acidification. Only the component of poly-C that was soluble in THF was collected (26% yield). Poly-A$_x$ was soluble in the common organic solvents, such as benzene, toluene, THF, $CHCl_3$, and pyridine, while the THF-soluble poly-C was also soluble in pyridine.

The chiral/achiral amidine copolymer compositions were determined from their ^{1}H NMR spectra. Figure 2 shows the partial ^{1}H NMR spectra of the phenylene linker protons of poly-A$_x$, which were sensitive to the sequences of the chiral and achiral amidine units. By comparing the chemical shifts for the homopolymers of the chiral (H_1: a in Figure 2) and achiral (H_3: f) amidines, the two new peaks observed for the chiral/achiral amidine copolymers (H_2: b–e) were unambiguously assigned to the nonequivalent phenylene linker protons between the chiral and achiral, or achiral and chiral amidine units. The upfield shifts of the H_1–H_3 protons can be ascribed to the ring current effect of the phenyl moieties at the chiral amidine units. The obtained chiral/achiral amidine copolymer compositions nearly

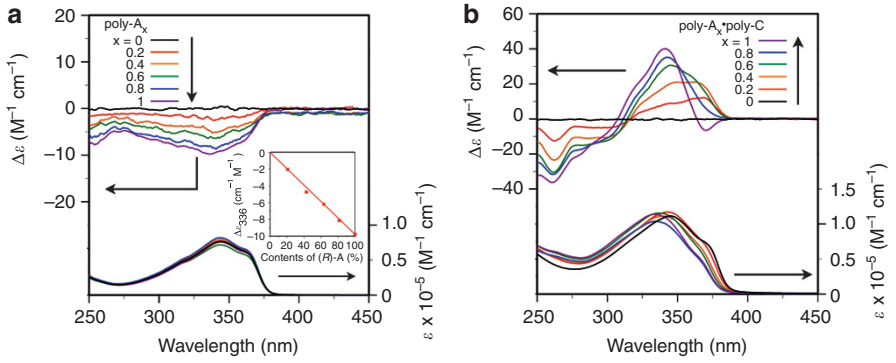

Figure 3 (**a**) CD and absorption spectra of poly-A$_x$ (0.1 mM per unit) in THF at 25 °C. The inset shows the plots of the CD intensity at 336 nm ($\Delta\varepsilon_{336}$) versus the contents of (*R*)-A. (**b**) CD and absorption spectra of equimolar mixtures of poly-A$_x$ and poly-C (0.1 mM per unit) in THF at 25 °C after reaching equilibrium (poly-A$_0$ · poly-C; 18 h, poly-A$_{0.2}$ · poly-C; 9 h, poly-A$_{0.4}$ · poly-C; 21 h, poly-A$_{0.6}$ · poly-C; 24 h, poly-A$_{0.8}$ · poly-C; 21 h, poly-A$_1$ · poly-C; 17 h).

agreed with those in the feed (Table 1), which suggests that the copolymerization mostly proceeded in a random manner.

The chiral amplification behavior in the double-helix formation was then evaluated by CD and absorption spectroscopies. First, we collected the CD and absorption spectra of the single-stranded poly-A$_x$ in THF at 25 °C (Figure 3a). As anticipated, poly-A$_x$ exhibited weak induced CDs in the π-conjugated backbone regions, and the CD and absorption spectra were similar in pattern regardless of the chiral/achiral amidine compositions. In addition, the CD intensities monotonically increased with increasing chiral amidine contents (see the inset in Figure 3a), which resulted in a linear relationship between the CD intensity at 336 nm and the chiral amidine contents. These results indicated a random conformation of poly-A$_x$; in other words, the chiral/achiral amidine copolymers, poly-A$_x$, have a non-helical structure in solution.

Next, the double-helix formation of poly-A$_x$ with poly-C was investigated in THF (Figure 3b). Upon mixing equimolar amounts of poly-A$_x$ ($x = 0.2$, 0.4, 0.6, and 0.8) and poly-C, the positive cotton effects, which are completely different from those of the chiral/achiral amidine copolymers, appeared in the absorption regions of the *p*-diethynylphenylene linkers, and the CD intensities gradually increased with time and reached constant values after *ca.* 9–24 h (Figure 3b), as observed for the double-helical poly-A$_1$ · poly-C,[29] which indicates that the poly-A$_x$ · poly-C duplexes ($x = 0.2$, 0.4, 0.6, and 0.8) most likely formed an excess single-handed double-helical structure through amidinium–carboxylate salt bridges. Interestingly, the poly-A$_x$ · poly-C duplexes showed an additional positive cotton effect in the longer wavelength regions, and their intensities tended to increase with the increasing achiral amidine contents. At the same time, the CD intensity centered at 341 nm decreased. These changes in the CD spectra were accompanied by a remarkable redshift in the absorption spectra; the absorption maximum of the poly-A$_x$ · poly-C duplexes shifted from 334 nm (poly-A$_1$ · poly-C; all-chiral amidine duplex) to 344 nm (poly-A$_0$ · poly-C; all-achiral amidine duplex). These results suggest that the absorption band, which appeared in the longer-wavelength regions, may be due to the *p*-diethynylphenylene linker chromophores associated with the achiral amidine units at which the cotton effects might be induced through a preferred-handed double-helix formation.

Based on these results, we attempted to subtract the chiral amidine components from the absorption and CD spectra of the poly-A$_x$ · poly-C duplexes in Figure 3b using those of the chiral amidine homopolymer complexed with poly-C (poly-A$_1$ · poly-C), which allowed us to extract the contribution of the achiral amidine units to their absorption and CD spectra. The subtracted absorption and CD spectra (Figure 4) were obtained by taking into account that the chiral amidine contents of the poly-A$_x$ · poly-C ($x = 0.2$, 0.4, 0.6, and 0.8) duplexes showed similar patterns and that the molar absorptivity at 345 nm (ε_{345}) and the achiral amidine contents in the poly-A$_x$ · poly-C duplexes showed a linear relationship (Figure 4, inset). These results suggest that the contributions of the achiral amidine units to their absorption and CD spectra may be evaluated once poly-A$_x$ is complexed with the complementary poly-C strand.

To quantitatively discuss the chirality transfer abilities of the chiral amidine units to the achiral ones along the double-helical polymer backbones, the relationships between the changes in the CD intensities at 367 nm that may reflect the preferred-handed double-helix formation of the achiral amidine units in poly-A$_x$ · poly-C (Figure 4) and the chiral amidine contents were simulated based on a diad sequence model.

The chiral/achiral amidine units are randomly distributed in each amidine copolymer independent of the feed molar ratios, which was confirmed by their ^{1}H NMR spectra (Figure 2); therefore, upon complexation with poly-C, there are four possible diad sequences along the double-helical polymer poly-A$_x$ · poly-C, that is, chiral–chiral (C–C), chiral–achiral (C–A), achiral–chiral (A–C) and achiral–achiral (A–A). The relative abundances of these diad segments are as follows:

$$\text{Chiral} - \text{Chiral}\,(\text{C}-\text{C}): \quad q^2$$

$$\text{Chiral} - \text{Achiral}\,(\text{C}-\text{A}): \quad q(1-q)$$

$$\text{Achiral} - \text{Chiral}\,(\text{A}-\text{C}): \quad (1-q)q$$

$$\text{Achiral} - \text{Achiral}\,(\text{A}-\text{A}): \quad (1-q)^2$$

where q ($0 \le q \le 1$) is the chiral amidine content in the poly-A$_x$ · poly-C. This diad model suggests that the C–C, C–A and A–C sequences can be CD active, while the A–A is CD silent (Figure 5).

The CD intensities at 367 nm in Figure 4, which result from the preferred-handed double-helix formation of the achiral amidine units in poly-A$_x$ · poly-C, can then be calculated on the basis of the following assumptions: (1) only the achiral amidine units lying next to the chiral amidine units (C–A and A–C) will exhibit an induced CD at 367 nm, and (2) the CD intensity induced at each achiral amidine unit is identical. The sum of the CD intensities for the achiral amidine units in poly-A$_x$ · poly-C ($\Delta\varepsilon_{\text{achiral}}$) at 367 nm is proportional to the number of achiral amidine units lying next to the chiral

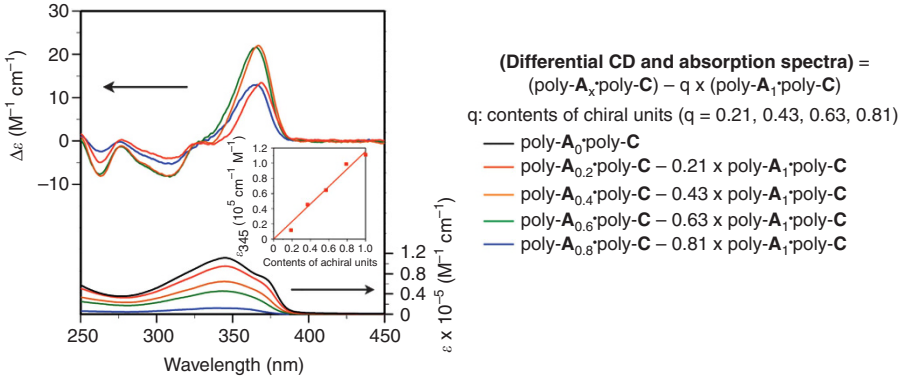

Figure 4 Differential CD and absorption spectra corresponding to the achiral amidine units in poly-A_x · poly-C ($x = 0.2$ (red), 0.4 (orange), 0.6 (green), and 0.8 (blue)) obtained by subtracting the CD and absorption spectra of the chiral amidine homopolymer complexed with poly-C (poly-A_1 · poly-C) from those of the poly-A_x · poly-C. Absorption spectrum of poly-A_0 · poly-C (black) is also shown for comparison. The inset shows the plots of the molar absorptivity at 345 nm (ε_{345}) versus the contents of the achiral amidine units.

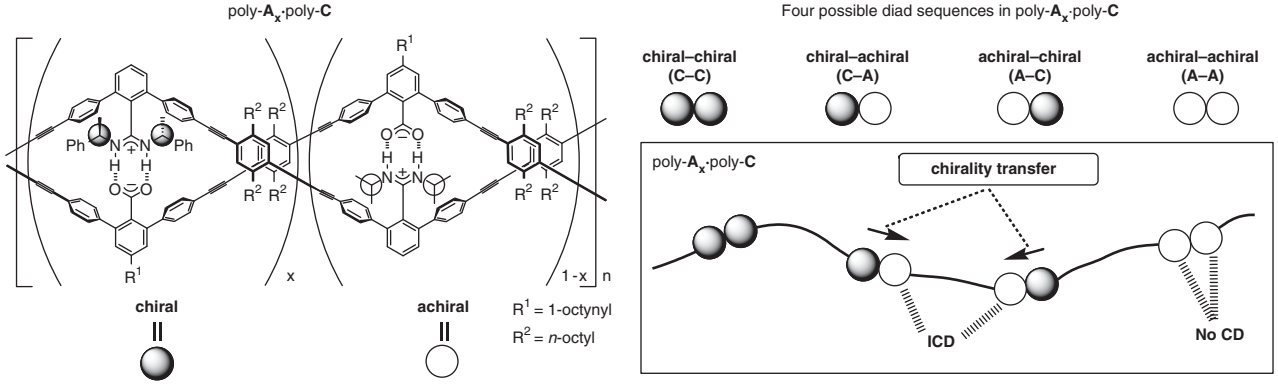

Figure 5 Schematic representation of the chiral–achiral amidine diad model.

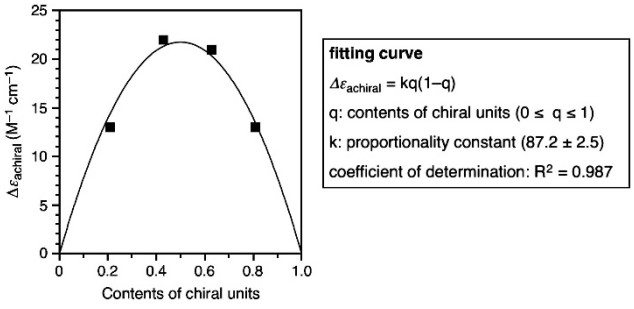

Figure 6 Plots of the differential CD intensity for the poly-A_x · poly-C duplexes ($x = 0.2$, 0.4, 0.6, and 0.8) at 367 nm versus the chiral amidine contents. The red curve represents the curve fitting results based on Equation (1) with $k = 87.2$.

amidine units. The $\Delta\varepsilon_{\text{achiral}}$ is then given by the following equation (1):

$$\Delta\varepsilon_{\text{achiral}} N(q(1-q)+(1-q)q) = kq(1-q) \quad (1)$$

where N and k are the total number of the diads in the poly-A_x · poly-C duplexes and the proportionality constant, respectively.

Figure 6 shows the plots of the differential CD intensities for the poly-A_x · poly-C duplexes at 367 nm versus the chiral amidine contents, revealing the maximum CD intensity at a chiral amidine content of *ca.* 0.5. The fit curve was obtained by the nonlinear least-squares method using Equation (1) with $k = 87.2$ and shows good agreement with the CD intensity changes at 367 nm, indicating that the chiral–achiral amidine diad model developed in this study well describes the chiral amplification behavior in poly-A_x · poly-C, that is, the chirality of the chiral amidine units certainly transfers to the achiral ones along the double-helical polymer backbones, at least when the achiral amidine lies next to the chiral amidine in the poly-A_x · poly-C duplexes. However, at this time, we have no information on the helical sense excesses of the poly-A_x · poly-C duplexes, and further discussion on the present amplification of the chirality is difficult.

CONCLUSION

In conclusion, we have synthesized a series of chiral/achiral amidine-based random copolymers with *m*-terphenylene backbones (poly-A_x) and found that the chiral/achiral amidine strands formed a double helix upon complexation with the complementary achiral carboxylic acid strand (poly-C) through amidinium–carboxylate salt bridges. The CD and absorption measurements of the poly-A_x and poly-A_x · poly-C duplexes revealed that the macromolecular helicity of the poly-A_x · poly-C duplex was definitely amplified by the chirality transfer from the chiral amidine residues to the adjacent achiral ones. In sharp contrast, no chiral amplification in the macromolecular helicity was observed for the chiral/achiral amidine single strands. Therefore, a further study on the structural analysis of the

poly-A_x · poly-C duplexes, for example, by high-resolution atomic force microscopy[29] is required to obtain more direct information dealing with the amplification of the helical chirality, that is, an excess handedness of the helical chirality, which may reveal to what extent the chirality of the amidine transfers to the achiral amidines through the duplex formation. However, we believe that the present finding will contribute to the design and construction of a wide variety of double-stranded helical polymers with a controlled helical structure assisted by chiral amplification.

ACKNOWLEDGEMENTS

This work was supported in part by a Grant-in-Aid for Scientific Research (S) from the Japan Society for the Promotion of Science (JSPS).

1 Lehn, J. M. *Supramolecular Chemistry: Concepts and Perspectives* (VCH, Weinheim, 1995).
2 Hill, D. J., Mio, M. J., Prince, R. B., Hughes, T. S. & Moore, J. S. A field guide to foldamers.. *Chem. Rev.* **101,** 3893–4011 (2001).
3 Yashima, E., Maeda, K., Iida, H., Furusho, Y. & Nagai, K. Helical polymers: synthesis, structures and functions.. *Chem. Rev.* **109,** 6102–6211 (2009).
4 Green, M. M., Park, J.-W., Sato, T., Teramoto, A., Lifson, S., Selinger, R. L. B. & Selinger, J. V. The macromolecular route to chiral amplification. *Angew. Chem. Int. Ed.* **38,** 3138–3154 (1999).
5 Nakano, T. & Okamoto, Y. Synthetic helical polymers: conformation and function. *Chem. Rev.* **101,** 4013–4038 (2001).
6 Aoki, T. & Kaneko, T. New macromolecular architectures for permselective membranes–Gas permselective membranes from dendrimers and enantioselectively permeable membranes from one-handed helical polymers. *Polym. J.* **37,** 717–735 (2005).
7 Fujiki, M. Mirror symmetry breaking of silicon polymers—from weak bosons to artificial helix. *Chem. Rec.* **9,** 271–298 (2009).
8 Hecht, S. & Huc, I. *Foldamers: Structure, Properties, and Applications* (WILEY–VCH, Weinheim, 2007).
9 Yashima, E., Maeda, K. & Furusho, Y. Single- and double-stranded helical polymers: synthesis, structures and functions. *Acc. Chem. Res.* **41,** 1166–1180 (2008).
10 Rudick, J. G. & Percec, V. Induced helical backbone conformations of self- organizable dendronized polymers. *Acc. Chem. Res.* **41,** 1641–1652 (2008).
11 Schwartz, E., Koepf, M., Kitto, J. H., Nolte, R. J. M. & Rowan, A. E. Helical poly(isocyanides): past, present and future. *Polym. Chem.* **2,** 33–47 (2011).
12 Shiotsuki, M., Sanda, F. & Masuda, T. Polymerization of substituted acetylenes and features of the formed polymers. *Polym. Chem.* **2,** 1044–1058 (2011).
13 Albrecht, M. 'Let's twist again'–Double-stranded, triple-stranded, and circular helicates. *Chem. Rev.* **101,** 3457–3497 (2001).
14 Huc, I. Aromatic oligoamide foldamers. *Eur. J. Org. Chem.* 17–29 (2004).
15 Furusho, Y. & Yashima, E Molecular design and synthesis of artificial double helices. *Chem. Rec.* **7,** 1–11 (2007).
16 Amemiya, R. & Yamaguchi, M. Chiral recognition in noncovalent bonding interactions between helicenes: right-handed helix favors right-handed helix over left-handed helix.. *Org. Biomol. Chem.* **6,** 26–35 (2008).
17 Haldar, D. & Schmuck, C. Metal-free double helices from abiotic backbones. *Chem. Soc. Rev.* **38,** 363–371 (2009).
18 Furusho, Y. & Yashima, E Development of synthetic double helical polymers and oligomers. *J. Polym. Sci. Part A: Polym. Chem.* **47,** 5195–5207 (2009).
19 Furusho, Y. & Yashima, E. Synthesis and function of double-stranded helical polymers and oligomers. *Macromol. Rapid Commun.* **32,** 136–146 (2011).
20 Guichard, G. & Huc, I. Synthetic foldamers. *Chem. Commun.* **47,** 5933–5941 (2011).
21 Yang, H.-C., Lin, S.-Y., Yang, H.-C., Lin, C.-L., Tsai, L., Huang, S.-L., Chen, I. W.-P., Chen, C.-h., Jin, B.-Y. & Luh, T.-Y. Molecular architecture towards helical double stranded polymers. *Angew. Chem. Int. Ed.* **45,** 726–730 (2006).
22 Goto, H., Katagiri, H., Furusho, Y. & Yashima, E. Oligoresorcinols fold into double helices in water. *J. Am. Chem. Soc.* **128,** 7176–7178 (2006).
23 Tanaka, Y., Katagiri, H., Furusho, Y. & Yashima, E. A modular strategy to artificial double helices. *Angew. Chem. Int. Ed.* **44,** 3867–3870 (2005).
24 Furusho, Y., Tanaka, Y., Maeda, T., Ikeda, M. & Yashima, E. Photoresponsive double-stranded helices composed of complementary strands. *Chem. Commun.* **30,** 3174–3176 (2007).
25 Hasegawa, T., Furusho, Y., Katagiri, H. & Yashima, E. Enantioselective synthesis of complementary double-helical molecules that catalyze asymmetric reactions. *Angew. Chem. Int. Ed.* **46,** 5885–5888 (2007).
26 Ito, H., Furusho, Y., Hasegawa, T. & Yashima, E. Sequence- and chain-length-specific complementary double-helix formation. *J. Am. Chem. Soc.* **130,** 14008–14015 (2008).
27 Iida, H., Shimoyama, M., Furusho, Y. & Yashima, E. Double-stranded supramolecular assembly through salt bridge formation between rigid and flexible amidine and carboxylic acid strands. *J. Org. Chem.* **75,** 417–423 (2010).
28 Ito, H., Ikeda, M., Hasegawa, T., Furusho, Y. & Yashima, E. Synthesis of complementary double-stranded helical oligomers through chiral and achiral amidinium—carboxylate salt bridges and chiral amplification in their double-helix formation. *J. Am. Chem. Soc.* **133,** 3419–3432 (2011).
29 Maeda, T., Furusho, Y., Sakurai, S.-I., Kumaki, J., Okoshi, K. & Yashima, E. Double-stranded helical polymers consisting of complementary homopolymers. *J. Am. Chem. Soc.* **130,** 7938–7945 (2008).
30 Palmans, A. R. A. & Meijer, E. W. Amplification of chirality in dynamic supramolecular aggregates. *Angew. Chem. Int. Ed.* **46,** 8948–8968 (2007).
31 Pijper, D. & Feringa, B. L. Control of dynamic helicity at the macro- and supramolecular level. *Soft Matter* **4,** 1349–1372 (2008).
32 Green, M. M., Reidy, M. P., Johnson, R. J., Darling, G., O'Leary, D. J. & Willson, G. Macromolecular stereochemistry: the out-of-proportion influence of optically active comonomers on the conformational characteristics of polyisocyanates. The sergeants and soldiers experiment. *J. Am. Chem. Soc.* **111,** 6452–6454 (1989).
33 Green, M. M., Peterson, N. C., Sato, T., Teramoto, A., Cook, R. & Lifson, S. A. Helical polymer with a cooperative response to chiral information. *Science* **268,** 1860–1866 (1995).
34 Okamoto, Y., Nishikawa, M., Nakano, T., Yashima, E. & Hatada, K. Induction of a single-handed helical conformation through radical polymerization of optically active phenyl-2-pyridyl-o-tolylmethyl methacrylate. *Macromolecules* **28,** 5135–5138 (1995).
35 Takei, F., Onitsuka, K. & Takahashi, S. Induction of screw-sense in poly(isocyanide)s by random copolymerization between chiral and achiral isocyanides using Pd-Pt μ-ethynediyl dinuclear complex as an Initiator. *Polym. J.* **32,** 524–526 (2000).
36 Nomura, R., Fukushima, Y., Nakako, H. & Masuda, T. Conformational study of helical poly(propiolic esters) in solution. *J. Am. Chem. Soc.* **122,** 8830–8836 (2000).
37 Prince, R. B., Moore, J. S., Brunsveld, L. & Meijer, E. W. Cooperativity in the folding of helical m-phenylene ethynylene oligomers based upon the 'sergeants-and-soldiers' principle. *Chem.–Eur. J.* **7,** 4150–4154 (2001).
38 Yue, D., Shiotsuki, M., Sanda, F. & Masuda, T. Copolymerization of N--propargylphosphonamidates. Helicity control of the copolymers by P-chirality. *Polymer* **48,** 68–73 (2007).
39 Deng, J., Luo, X., Zhao, W. & Yang, W. A novel type of optically active helical polymers: synthesis and characterization of poly(N-propargylureas). *J. Polym. Sci. Part A: Polym. Chem.* **46,** 4112–4121 (2008).
40 Mateos-Timoneda, M. A., Crego-Calama, M. & Reinhoudt, D. N. Supramolecular chirality of self-assembled systems in solution. *Chem. Soc. Rev.* **33,** 363–372 (2004).
41 Maeda, K. & Yashima, E. Dynamic helical structures: detection and amplification of chirality. *Top. Curr. Chem.* **265,** 47–88 (2006).
42 Yamamoto, T., Fukushima, T., Kosaka, A., Jin, W., Yamamoto, Y., Ishii, N. & Aida, T. Conductive one-handed nanocoils by coassembly of morphology and helical chirality. *Angew. Chem. Int. Ed.* **47,** 1672–1675 (2008).
43 Wilson, A. J., Gestel, J., Sijbesma, R. P. & Meijer, E. W. Amplification of chirality in benzene tricarboxamide helical supramolecular polymers. *Chem. Commun.* 4404–4406 (2006).
44 Praveen, V. K., Babu, S. S., Vijayakumar, C., Varghese, R. & Ajayaghosh, A. Helical supramolecular architectures of self-assembled linear π-systems. *Bull. Chem. Soc. Jpn.* **81,** 1196–1211 (2008).
45 Wittung, P., Eriksson, M., Lyng, R., Nielsen, P. E. & Nordén, B. Induced chirality in PNA-PNA duplexes. *J. Am. Chem. Soc.* **117,** 10167–10173 (1995).
46 Totsingan, F., Jain, V., Bracken, W. C., Faccini, A., Tedeschi, T., Marchelli, R., Corradini, R., Kallenbach, N. R. & Green, M. M. Conformational heterogeneity in PNA:PNA duplexes. *Macromolecules* **43,** 2692–2703 (2010).
47 Gan, Q., Li, F., Li, G., Kauffmann, B., Xiang, J., Huc, I. & Jiang, H. Heteromeric double helix formation by cross-hybridization of chloro-and fluoro-substituted quinoline oligoamides. *Chem. Commun.* **46,** 297–299 (2010).